CONTRIBUTION FROM THE METCALF RESEARCH LABORATORY, DEPARTMENT OF CHEMISTRY, BROWN UNIVERSITY, PROVIDENCE, RHODE ISLAND 02912

Spectroscopic Studies of Metal–Metal Bonding. V. Direct and Indirect Intermetallic Forces from the Vibrational Spectra and Analyses of $M_2Cl_9^{3-}$ (M = Cr, W) Ions[1]

BY ROBERT J. ZIEGLER AND WILLIAM M. RISEN, JR.*[2]

Received April 5, 1972

The infrared and laser Raman spectra of the $M_2Cl_9^{3-}$ (M = Cr, W) complex ions are reported, and all observed fundamentals in the spectra of $Cs_3Cr_2Cl_9$, $(Et_4N)_3Cr_2Cl_9$, $(Bu_4N)_3Cr_2Cl_9$, $K_3W_2Cl_9$, $Cs_3W_2Cl_9$, and $(Bu_4N)_3W_2Cl_9$ are assigned on the basis of exact or approximate D_{3h} symmetry. Vibrational normal coordinate analyses for the complex ions in $Cs_3Cr_2Cl_9$ and $K_3W_2Cl_9$ are reported which yield excellent agreement between calculated and assigned spectra and which are based on both reasonable spectroscopic assumptions and a general symmetrized valence force field. Contributions of the M–Cl_b–M and Cl_b–M–Cl_b deformations of the tri-μ-chloro-dimetalate unit to the molecular force field of the $Cr_2Cl_9^{3-}$ ion are assessed assuming no direct Cr–Cr interaction and are then transferred exactly to the molecular force field of the $W_2Cl_9^{3-}$ ion. The direct W–W interaction is then determined by fitting the calculated to the observed spectra. The tungsten–tungsten stretching force constant, k_{W-W}, is calculated to be 1.15 ± 0.1 mdyn/Å. The vibrational eigenvectors and potential energy distribution show that this force field element contributes significantly to several of the A_1' vibrational modes, and they are analyzed to develop the basis for treating metal cluster species of the M_6X_8 and M_6X_{12} types.

Introduction

The analysis of the vibrational spectrum of simple bi- and polynuclear metal complexes as a means of determining the nature of their metal–metal interactions continues to be an area of active research in this laboratory[3] as well as in many others.[4] However, the majority of systems analyzed to date have been of complexes having unsupported metal–metal bonds, and the contribution of this type of metal–metal interaction to the molecular force field has, therefore, been relatively easy to assess. If the calculations of such forces in simple systems are to be used to investigate the strength of the metal–metal interactions in metals and alloys, which cannot accurately be approximated as unsupported one-dimensional chains, the model systems chosen for spectroscopic analysis must include those in which the metal–metal bonds form a lattice-like array. Obvious choices for such model systems are the cluster species containing the M_6X_8 and M_6X_{12} structural units which are characterized by an octahedral arrangement of the metal atoms. Here, however, the molecular force field is complicated by the presence of bridging halogen atoms as well as "bridging" metal atoms and the need to assess the relative contribution of the former to the force field becomes apparent.

The binuclear anions $M_2X_9^{3-}$ (M = Cr, W; X = Cl, Br) provide a set of complexes in which the contribution of the bridging halogen atoms to a molecular force field, which includes a direct metal–metal interaction, can be assessed. The $Cr_2Cl_9^{3-}$ and $Cr_2Br_9^{3-}$ ions, as characterized by X-ray structure determinations,[5,6] consist of two face-shared octahedra in which the chromium atoms are displaced outward along the Cr–Cr axis from the centers of their respective octahedra. The effect of increasing the size of the cation[7] from K^+ to Et_4N^+ is to further increase the Cr–Cr separation and, accordingly, increase the Cr–X_b–Cr angle. Further evidence of the absence of a direct Cr–Cr interaction in $Cr_2X_9^{3-}$ is provided by its electronic absorption spectrum[8-10] which closely resembles that of the CrX_6^{3-} ions, and its bulk paramagnetism[7-9] which approximates that of a Cr(III) ion (d^3) with three unpaired electrons.

Quite contrary behavior is observed in the isostructural $W_2Cl_9^{3-}$ ion where an X-ray study[11] has shown that the bioctahedron is considerably squashed along the W–W internuclear axis with a W–W separation less than that found in metallic tungsten and essentially unaffected by the size of the cation.[10] The indication of a very strong W–W bonding interaction in the $W_2Cl_9^{3-}$ ion is further supported by its near diamagnetism,[5,12] and the disparity between the observed electronic spectra[10,13-15] of the $W_2X_9^{3-}$ ions and that expected for the hypothetical WX_6^{3-} ions.

We have taken the approach of measuring and analyzing the vibrational spectra of the $Cr_2Cl_9^{3-}$ and $W_2Cl_9^{3-}$ ions in attempting to investigate the relationship between direct and indirect intermetallic interactions. Based on the solution of the force field for the chromium complex using a metal–metal force constant of essentially zero, the values for the various deformation forces involved in the bridging unit can then be transferred to the force field for the tungsten complex to determine the value of k_{W-W} and the force field partitioning within the assumed approach. Our results of this investigation are presented below.

(1) Abstracted in part from the Ph.D. Thesis of R. J. Ziegler, Brown University, 1972.

(2) Author to whom correspondence should be addressed.

(3) (a) K. L. Watters, J. N. Brittain, and W. M. Risen, Jr., *Inorg. Chem.*, **8**, 1347 (1969); (b) K. L. Watters, W. M. Butler, and W. M. Risen, Jr., *ibid.*, **10**, 1970 (1971); (c) R. J. Ziegler, J. M. Burlitch, S. E. Hayes, and W. M. Risen, Jr., *ibid.*, **11**, 702 (1972); (d) J. R. Johnson, R. J. Ziegler, and W. M. Risen, Jr., to be submitted.

(4) K. L. Watters and W. M. Risen, Jr., *Inorg. Chim. Acta Rev.*, **3**, 129 (1969).

(5) G. J. Wessel and D. J. W. Ijdo, *Acta Crystallogr.*, **10**, 466 (1957).

(6) R. Saillant, R. B. Jackson, W. E. Streib, K. Folting, and R. A. D. Wentworth, *Inorg. Chem.*, **10**, 1453 (1971).

(7) I. E. Grey and P. W. Smith, *Aust. J. Chem.*, **24**, 73 (1971).

(8) R. Saillant and R. A. D. Wentworth, *Inorg. Chem.*, **7**, 1606 (1968).

(9) P. C. Crouch, G. W. A. Fowles, and R. A. Walton, *J. Chem. Soc. A*, 972 (1969).

(10) P. W. Smith and A. G. Wedd, *ibid.*, 2447 (1970).

(11) W. H. Watson, Jr., and J. Waser, *Acta Crystallogr.*, **11**, 689 (1958).

(12) W. Klemm and H. Steinberg, *Z. Anorg. Allg. Chem.*, **227**, 193 (1936).

(13) R. Saillant, J. L. Hayden, and R. A. D. Wentworth, *Inorg. Chem.*, **6**, 1497 (1967).

(14) J. L. Hayden and R. A. D. Wentworth, *J. Amer. Chem. Soc.*, **90**, 5291 (1968).

(15) J. Lewis, R. S. Nyholm, and P. W. Smith, *J. Chem. Soc. A*, 57 (1969).

TABLE I

OBSERVED INFRARED AND RAMAN SPECTRA OF THE $Cr_2Cl_9^{3-}$ AND $W_2Cl_9^{3-}$ COMPLEX IONS[a]

Raman, cm^{-1}	Rel intens	Ir, cm^{-1}	Rel intens	Symmetry (D_{3h})	Assignment
			$Cs_3Cr_2Cl_9$		
		398	mw	$A_2'' \times E''$	$\nu_9 + \nu_{16}$
				$E' \times E''$	$\nu_{14} + \nu_{15}$
375	15			A_1'	ν_1
		369	w, sh	$A_2'' \times E''$	$\nu_8 + \nu_{18}$
				$E' \times E'$	$\nu_{11} + \nu_{13}$
363	9			$(A_2'')^2$	$2\nu_9$
				$E' \times E'$	$\nu_{11} + \nu_{17}$
		360	vs	A_2''	ν_7
335	3	342	vs	E'	ν_{10}
320	5			E''	ν_{15}
		319	w, sh	$E' \times E''$	$\nu_{12} + \nu_{17}$
280	28			A_1'	ν_2
		261	s	A_2''	ν_8
233	20	234	m	E'	ν_{11}
222	2			E''	ν_{16}
196	12	196	mw	E'	ν_{12}
		184	m	A_2''	ν_9
180	2			$E'' \times E''$	$\nu_{15} - \nu_{17}$
				$E' \times E''$	$\nu_{15} - \nu_{13}$
172	1			$A_1' \times E'$	$\nu_1 - \nu_{12}$
				$A_2'' \times A_2''$	$\nu_7 - \nu_9$
161	20			A_1'	ν_3
		158	w	$(E')^2$	$2\nu_{14}$
143	10	138	mw	E'	ν_{18}
138	10				
131	1			E''	ν_{17}
121	1			A_1'	ν_4
113	1			E''	ν_{18}
		111	w, sh	$E' \times E'$	$\nu_{12} - \nu_{14}$
				$A_1' \times A_2''$	$\nu_1 - \nu_8$
				$A_1' \times E'$	$\nu_{11} - \nu_4$
		103	w, sh	$E' \times E'$	$\nu_{10} - \nu_{11}$
				$E' \times E''$	$\nu_{11} - \nu_{17}$
~78[c]	5	80	vs, br	E'	ν_{14}
		57	mw		Lattice?
		45	mw		Lattice?
			$(Et_4N)_3Cr_2Cl_9$[b]		
		343	vs	A_2''	ν_7
		319	vs	E'	ν_{10}
		300	w, sh		
		284	w		
		266	m	A_2''	ν_8
		203	w	E'	ν_{12}
		175	w	A_2''	ν_9
		139	w	E'	ν_{13}
		123	w		
		103	w, sh		
		97	w, sh		
		89	ms, br	E'	ν_{14}
		84	m, sh		
		72	mw		
		61	w		Lattice?
		49	m		Lattice?
			$(Bu_4N)_3Cr_2Cl_9$		
364	5			$A_1' \times A_1'$	$\nu_2 + \nu_4$
				$E' \times E'$	$\nu_{11} + \nu_{13}$
350	45			A_1'	ν_1
		344	vs, br	A_2''	ν_7
343	10			$(A_2'')^2$	$2\nu_9$
				$A_1' \times E'$	$\nu_3 + \nu_{12}$
				$E' \times E''$	$\nu_{11} + \nu_{17}$
333	25			$A_1' \times E'$	$\nu_4 + \nu_{11}$
				$E' \times E''$	$\nu_{11} + \nu_{18}$
316	35	315	vs, br	E'	ν_{10}
297	65			E''	ν_{15}
		292	w, sh	$A_1' \times E'$	$\nu_4 + \nu_{12}$
				$E' \times E''$	$\nu_{12} + \nu_{18}$
268	10			A_1'	ν_2
		267	ms	A_2''	ν_8
243	50	233	w	E'	ν_{11}
222	20			E''	ν_{16}
197	50	202	w	E'	ν_{12}
		174	ms	A_2''	ν_9
165	5			$A_1' \times A_1'$	$\nu_2 - \nu_4$
				$A_1' \times E'$	$\nu_{10} - \nu_3$
				$A_2'' \times A_2''$	$\nu_7 - \nu_9$
158	15			$A_1' \times E''$	$\nu_2 - \nu_{17}$
				$E' \times E'$	$\nu_{11} - \nu_{14}$
147	60			A_1'	ν_8
127	50	130	m	E'	ν_{13}
110	50			E''	ν_{17}
		104	w, sh	$E' \times E'$	$\nu_{11} - \nu_{13}$
100	40			A_1'	ν_4
96	40			E''	ν_{18}
~80[c]	40	82	s, br	E'	ν_{14}
		70	w, sh	$A_1' \times A_2''$	$\nu_9 - \nu_4$
				$A_1' \times E'$	$\nu_2 - \nu_{12}$
				$E' \times E'$	$\nu_{12} - \nu_{13}$
63	30				Lattice?
			$K_3W_2Cl_9$		
332	45			A_1'	ν_1
316	2			$(A_2'')^2$	$2\nu_9$
				$A_1' \times E'$	$\nu_3 + \nu_{12}$
		313	vs	A_2''	ν_7
294	90			E''	ν_{15}
281	5	285	w	E'	ν_{10}
257	12			A_1'	ν_2
226	5			E''	ν_{16}
209	170	215	m	E'	ν_{11}
189	12			$A_1' \times E'$	$\nu_4 + \nu_{14}$
				$A_1' \times A_1'$	$\nu_1 - \nu_3$
				$(E')^2$	$2\nu_{13}$
178	10	181	m	E'	ν_{12}
162	10			$A_1' \times E'$	$\nu_{10} - \nu_4$
				$A_1' \times E'$	$\nu_2 - \nu_{13}$
				$E' \times E'$	$\nu_{13} + \nu_{14}$
		158	ms	A_2''	ν_9
139	210			A_1'	ν_3
123	10			E''	ν_{17}
115	10			A_1'	ν_4
107	15			E''	ν_{18}
91	7	96	ms	E'	ν_{13}
~76[c]	20	76	m	E'	ν_{14}
		51	w		Lattice?
			$Cs_3W_2Cl_9$		
		377	vw	$E' \times E'$	$\nu_{10} + \nu_{13}$
				$E' \times E'$	$\nu_{11} + \nu_{12}$
344	5			$A_1' \times E'$	$\nu_3 + \nu_{11}$
330	20			A_1'	ν_1
		313	vs	A_2''	ν_7
301	42			E''	ν_{15}
279	2	282	w	E'	ν_{10}
		232	mw	A_2''	ν_8
207	80	216	m	E'	ν_{11}
174	4	169	m	E'	ν_{12}
		152	ms	A_2''	ν_9
141	95			A_1'	ν_3
89	4	95	ms	E'	ν_{13}
~75[c]	9	71	s	E'	ν_{14}
		54	m		Lattice?
			$(Bu_4N)_3W_2Cl_9$[b]		
		311	vs	A_2''	ν_7
		289	vs	E'	ν_{10}
		274	w, sh		
		216	m	E'	ν_{11}
		171	m	E'	ν_{12}
		155	ms	A_2''	ν_9
		142	w, sh		
		101	m, br	E'	ν_{13}
		75	m	E'	ν_{14}

[a] All frequencies obtained from solid-state spectra. [b] Infrared spectra only. [c] Partially obscured by spurious line from spectrometer.

Experimental Section

The compounds of $M_2Cl_9^{3-}$ (M = Cr, W) employed in this investigation were prepared according to the following reported preparative procedures: $K_3W_2Cl_9$,[13,16] $Cs_3W_2Cl_9$,[15] $Cs_3Cr_2Cl_9$,[8] $(Et_4N)_3Cr_2Cl_9$,[17] and $(Bu_4N)_3Cr_2Cl_9$.[6] $(Bu_4N)_3W_2Cl_9$ was prepared in a manner analogous to $Cs_3W_2Cl_9$.

Samples for spectroscopic studies were prepared and handled in a dry nitrogen atmosphere when necessary to prevent decomposition. Infrared spectra were recorded as Nujol mulls between high-density polyethylene windows or as hot-pressed polyethylene pellets. Raman spectra were obtained from powdered samples sealed in melting point capillaries and from thick Nujol pastes under a nitrogen atmosphere in a specially designed cell to be described in a future paper.[18] Both the chromium and tungsten complexes are poor Raman scatterers and Raman bands attributable to the complex ions could be observed only for powered solid samples, and not in the spectra of solutions (*e.g.*, $(Bu_4N)_3Cr_2Cl_9$ in CH_2Cl_2 or $K_3W_2Cl_9$ in H_2O) or oil dispersions.[19] This precluded Raman polarization measurements. All observed vibrational frequencies were obtained from solid samples and are independent of the solid sampling technique employed.

The infrared spectra were recorded on a Beckman IR-11 spectrophotometer with a resolution of *ca.* 1 cm^{-1} and were calibrated against atmospheric water vapor absorption with the results of Blaine.[20] The laser Raman spectra were recorded on a Jarrell-Ash 25-300 laser Raman system with an accuracy of *ca.* 2 cm^{-1}. The 488.0 and 514.5 nm lasing lines of a Carson Model 150 FB Ar^+ laser were used to obtain the Raman spectra of the bluish purple chromium and green tungsten compounds, respectively. Where necessary, to eliminate sample decomposition, neutral density filters were used to reduce the power of the lasing lines. For all Raman spectra, the spectral slit widths were such that a resolution of *ca.* 5 cm^{-1} was maintained. The laser Raman spectrometer was calibrated against helium and neon emission lines.

Results

The complete vibrational spectra of the compounds $Cs_3Cr_2Cl_9$, $(Bu_4N)_3Cr_2Cl_9$, $K_3W_2Cl_9$, and $Cs_3W_2Cl_9$, the infrared spectra of the compounds $(Et_4N)_3Cr_2Cl_9$ and $(Bu_4N)_3W_2Cl_9$, and the assignments of all the observed fundamentals for each compound are presented in Table I. Previous reports of the vibrational spectra of the $Cr_2Cl_9^{3-}$ [9,17,21,22] and $W_2Cl_9^{3-}$ [23] ions, which have included only the infrared active metal–chlorine stretching modes occurring above 200 cm^{-1}, are generally in agreement with the results of this work. Complete spectral data including single-crystal Raman spectra and assignments have been reported for the isostructural $Cs_3Tl_2Cl_9$,[24] and the complete infrared spectrum of $(Et_4N)Ti_2Cl_9$ has also been reported.[25]

The molecular symmetry of the $M_2Cl_9^{3-}$ ions as determined by X-ray structural studies of $Cs_3Cr_2Cl_9$[5] and $K_3W_2Cl_9$[11] is D_{3h}. A far-infrared (400–200 cm^{-1}) spectral investigation[21] of the $Cr_2Cl_9^{3-}$ and $Mo_2Cl_9^{3-}$ complex ions as a function of cation has demonstrated that the vibrational band splittings resulting from the lowering of the site symmetry of the complexes are small enough to adopt approximate D_{3h} symmetry. We have, therefore, chosen to adopt D_{3h} symmetry for both $Cr_2Cl_9^{3-}$ and $W_2Cl_9^{3-}$ throughout this analysis.

The vibrational representation of these ions in D_{3h} symmetry is $\Gamma_{vib} = 4A_1' (R, pol) + 1A_1'' (ia) + 1A_2' (ia) + 3A_2'' (ir) + 5 E' (ir; R, depol) + 4 E'' (R, depol)$ (ir, infrared active; R, Raman active; ia, inactive; pol, polarized; depol, depolarized). The 27 internal normal modes occur as 18 vibrational fundamentals of which 16 are either infrared or Raman active. The distribution of the 16 active fundamentals among the symmetry coordinates generated by standard group theoretical techniques is listed in Table II. A representation of the molecular geometry and a labeling of the internal coordinates is shown in Figure 1.

TABLE II
DISTRIBUTION OF $M_2Cl_9^{3-}$ NORMAL MODES IN D_{3h} LOCAL SYMMETRY

	A_1'	A_1''	A_2'	A_2''	E′	E″
$\nu(M-Cl_t)$	1			1	1	1
$\nu(M-Cl_b)$	1			1	1	1
$\delta(Cl_b-M-Cl_t)$	1	1	1	1	2	2
$\delta(Cl_b-M-Cl_b)$	1			1[c]	1	1[c]
$\delta(M-Cl_b-M)$	1[a]				1[c]	
$\nu(M-M)$	1[b]					
Redundancies	2			1	1	1

[a] Forms a redundant coordinate with $\delta(Cl_b-M-Cl_b)$ of the same symmetry. [b] Was not included in the analysis of $Cr_2Cl_9^{3-}$. Forms a redundant coordinate with $\nu(M-Cl_b)$ and $\delta(Cl_b-M-Cl_b)$ in the analysis of $W_2Cl_9^{3-}$. [c] Forms a redundant coordinate with $\nu(M-Cl_b)$ of the same symmetry.

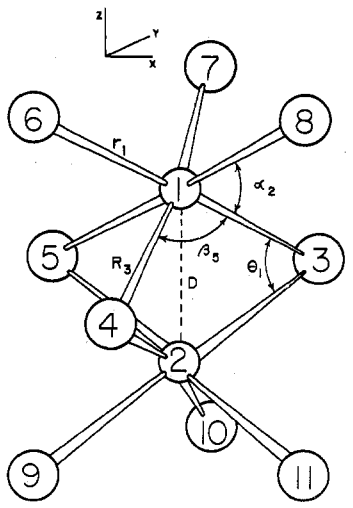

Figure 1.—The structure of the $M_2Cl_9^{3-}$ ions, showing the atomic numbering scheme and the internal coordinate-type definitions.

Spectral Assignments.—Theoretically, coincidences in the infrared and Raman spectra together with Raman polarization data permit the unambiguous assignment of the symmetry species of all 16 active fundamentals. Since Raman polarization data were not obtainable, consideration of infrared–Raman coincidences, partial grouping of the frequencies of the observed bands, and the results of the complete vibrational analysis of the isostructural $Cs_3Tl_2Cl_9$[24] were employed in making the spectral assignments. The observed vibrational spectra of $Cs_3Cr_2Cl_9$, $K_3W_2Cl_9$, and $Cs_3Tl_2Cl_9$ are correlated in Figure 2. The Raman spectrum of $K_3W_2Cl_9$ is presented in Figure 3 at several

(16) R. A. Laudise and R. C. Young, *Inorg. Syn.*, **6**, 149 (1960).
(17) D. M. Adams, J. Chatt, J. M. Davidson, and J. Gerratt, *J. Chem. Soc.*, 2189 (1963).
(18) R. J. Ziegler and W. M. Risen, Jr., *Appl. Spectrosc.*, to be submitted.
(19) B. J. Bulkin, *J. Opt. Soc. Amer.*, **59**, 1387 (1969).
(20) (a) L. R. Blaine, *J. Res. Nat. Bur. Stand., Sect. C*, **67**, 207 (1963); (b) L. R. Blaine, E. K. Plyler, and W. S. Benedict, *J. Res. Nat. Bur. Stand., Sect. A*, **66**, 223 (1962).
(21) I. E. Grey and P. W. Smith, *Aust. J. Chem.*, **22**, 1627 (1969).
(22) R. A. Work, III, and M. L. Good, *Inorg. Chem.*, **9**, 956 (1970).
(23) R. Saillant and R. A. D. Wentworth, *J. Amer. Chem. Soc.*, **91**, 2174 (1969).
(24) I. R. Beattie, T. R. Gilson, and F. A. Ozin, *J. Chem. Soc. A*, 2765 (1968).
(25) J. A. Creighton and J. H. S. Green, *ibid.*, 808 (1968).

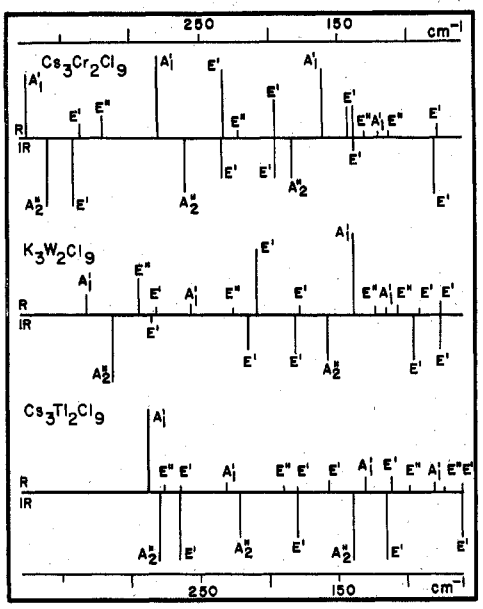

Figure 2.—Correlation diagram for the vibrational (ir and Raman) spectra of $Cs_3Cr_2Cl_9$, $K_3W_2Cl_9$, and $Cs_3Tl_2Cl_9$. $Cs_3Tl_2Cl_9$ data from ref 24.

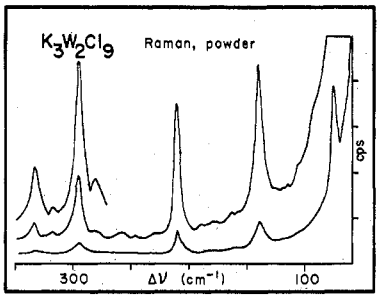

Figure 3.—The laser Raman spectrum of $K_3W_2Cl_9$ (powdered solid), presented at several spectral sensitivities to illustrate band shapes and relative intensities.

spectral sensitivities to illustrate band shapes and relative intensities.

Although all 16 active fundamentals are expected to appear in a relatively narrow spectral region (<400 cm^{-1}), the assignments of the observed spectra are aided by a partial grouping of the observed bands. From Table II, the bands due primarily to terminal chlorine–metal stretching vibrations (2 ir, 3 R) should appear at highest energy followed by a similar group of bands assignable primarily to the bridge chlorine–metal stretching modes (2 ir, 3 R). These should be followed by bands due mainly to the bending and deformation modes of the metal–terminal chlorine groups (3 ir, 5 R) and metal–bridge chlorine unit (1 ir, 2 R). As noted in Table II, the A_1' bridging deformation can be correlated to the redundant W–W stretching coordinate in the $W_2Cl_9^{3-}$ ion.

The $Cr_2Cl_9^{3-}$ Ion.—In the infrared and Raman spectra of $Cs_3Cr_2Cl_9$ the expected grouping of vibrational frequencies discussed above is observed, along with infrared–Raman coincidences assignable to internal modes of E′ symmetry. On the basis of these coincidences, the bands at 342, 234, 196, 138, and 80 cm^{-1} are all assigned as modes ν_{10} through ν_{14} of E′ symmetry. The infrared bands observed at 360, 261, and 184 cm^{-1} must be assigned, in D_{3h}, to the infrared active fundamentals ν_7 through ν_9 of A_2'' symmetry. The A_2'' modes of $Cs_3Cr_2Cl_9$ are generally more intense than the corresponding E′ modes, as in the case of $Cs_3Tl_2Cl_9$.[24] Since there is no significant Tl–Tl bonding in $Tl_2Cl_9^{3-}$, we may expect such similarities between its spectrum and that of $Cr_2Cl_9^{3-}$.

The Raman spectrum of $Cs_3Cr_2Cl_9$ is also similar to that of $Cs_3Tl_2Cl_9$ with both showing a similar intensity pattern and grouping of frequencies. The strongest band of each "group" of bands is assigned to the modes of A_1' symmetry and in $Cs_3Cr_2Cl_9$ these are observed at 375, 280, 161, and 121 cm^{-1} (ν_1–ν_4, respectively). The remainder of the Raman-active fundamentals, of E″ symmetry (ν_{15}–ν_{18}), are then assigned to bands observed at 320, 222, 131, and 113 cm^{-1}.

The observed infrared spectra of $(Et_4N)_3Cr_2Cl_9$ and $(Bu_4N)_3Cr_2Cl_9$ and Raman spectrum of the latter are very similar to those of $Cs_3Cr_2Cl_9$ and the assignments listed in Table I have been made on this basis. Our assignment of ν_{11} at 234 cm^{-1} in the Cs^+ salt and ~240 cm^{-1} in the $(Bu_4N)^+$ salt would appear to refute Grey and Smith's[21] tentative assignment of ν_{11} at 264 cm^{-1} in the $(Et_4N)^+$ salt. We do not observe a band assignable to ν_{11} in the $(Et_4N)^+$ salt and conclude that its intensity is too low to make it observable.

The $W_2Cl_9^{3-}$ Ion.—The vibrational spectrum of this complex ion was assigned, as listed in Table I, on the basis of infrared–Raman coincidences and the expected similarity in the energy ordering between bands observed in the spectra of the $W_2Cl_9^{3-}$ ion and analogous bands observed and assigned in the spectra of the $Cr_2Cl_9^{3-}$ ion and $Cs_2Tl_2Cl_9$.[24]

Thus, of those bands assignable to modes of primarily terminal chlorine–tungsten stretching vibrations observed in the spectrum of $K_3W_2Cl_9$, the infrared band at 285 cm^{-1}, coincident with the 281-cm^{-1} Raman band, is assigned to the E′ mode ν_{10}, and the strong infrared band at 313 cm^{-1} is thus assigned to the A_2'' mode ν_7. The Raman band at 332 cm^{-1} is assigned to the A_1' (ν_1) mode and that at 294 cm^{-1} to the E″ (ν_{15}) mode. This latter energy ordering is the same as that observed for the $Tl_2Cl_9^{3-}$ ion and indicates that the presence of the tungsten–tungsten interaction in the molecular force field, the normal vibration of which is symmetry allowed to couple with the A_1' terminal chlorine–tungsten stretching vibration, does not significantly affect the terminal M–Cl mode pattern.

A similar energy ordering is observed for those bands primarily due to bridge chlorine–tungsten stretching modes. For this "group," the highest frequency Raman band observed at 257 cm^{-1} is assigned to the A_1' mode ν_2. The Raman band observed at 226 cm^{-1} is assigned to the E″ mode ν_{16}. No band corresponding to ν_8 was observed in the infrared spectrum of $K_3W_2Cl_9$, but a weak band was observed in the infrared spectrum of $Cs_3W_2Cl_9$ at 232 cm^{-1} and is assigned accordingly. The strong Raman band at 209 cm^{-1} and the infrared band at 215 cm^{-1} are then assigned to the E′ mode ν_{11}.

The three remaining coincident E′ modes (ν_{12}–ν_{14}) are assigned to the infrared bands observed at 181 (178, R), 96 (91, R), and 76 cm^{-1}, and the infrared band at 158 cm^{-1} is assigned to the A_2'' mode (ν_9). The three weak Raman bands observed at 123, 115, and 107 cm^{-1} are assigned to modes of E″ (ν_{17}), A_1' (ν_4), and E″ (ν_{18}) symmetry, respectively, by direct analogy with

TABLE III
DEFINITION OF INTERNAL COORDINATES, S_j[a]

S_j	Description[b]	Atom No. Defining S_j[c]	S_j	Description[b]	Atom No. Defining S_j[c]	S_j	Description[b]	Atom No. Defining S_j[c]
S_1	r_1	1-6	S_{12}	R_6	2-5	S_{23}	α_{11}	5-2-9
S_2	r_2	2-9	S_{13}	α_1	3-1-7	S_{24}	α_{12}	5-2-10
S_3	r_3	1-7	S_{14}	α_2	3-1-8	S_{25}	β_1	4-1-5
S_4	r_4	2-10	S_{15}	α_3	3-2-10	S_{26}	β_2	4-2-5
S_5	r_5	1-8	S_{16}	α_4	3-2-11	S_{27}	β_3	5-1-3
S_6	r_6	2-11	S_{17}	α_5	4-1-8	S_{28}	β_4	5-2-3
S_7	R_1	1-3	S_{18}	α_6	4-1-6	S_{29}	β_5	3-1-4
S_8	R_2	2-3	S_{19}	α_7	4-2-11	S_{30}	β_6	3-2-4
S_9	R_3	1-4	S_{20}	α_8	4-2-9	S_{31}	θ_1	1-3-2
S_{10}	R_4	2-4	S_{21}	α_9	5-1-6	S_{32}	θ_2	1-4-2
S_{11}	R_5	1-5	S_{22}	α_{10}	5-1-7	S_{33}	θ_3	1-5-2
						S_{34}	D	1-2

[a] All bending coordinates were weighted by $(l_1 l_2)^{1/2}$ where l_1 and l_2 are the lengths of the sides defining the angle. [b] r_i = M–Cl_t stretch, R_i = M–Cl_b stretch, α_i = Cl_b–M–Cl_t deformation, β_i = Cl_b–M–Cl_b deformation, and θ_i = M–Cl_b–M deformation. [c] Refer to Figure 1 for numbering of atoms.

similar assignments made for the $Cr_2Cl_9^{3-}$ ion. Finally, the very strong Raman band observed at 139 cm^{-1} is assigned to the A_1' (ν_3) "accordion-type" deformation mode which must involve a large degree of tungsten–tungsten bond stretch.

Normal-Coordinate Analysis.—The procedure employed in the normal-coordinate analysis of the $M_2Cl_9^{3-}$ ions was to solve the vibrational eigenvalue problem for the $Cr_2Cl_9^{3-}$ ion first, using the Wilson GF matrix method[26] and symmetrized matrices, and then to transfer elements of the $Cr_2Cl_9^{3-}$ symmetrized force field associated with the deformation of the bridge structure to the $W_2Cl_9^{3-}$ symmetrized force field to permit its determination.

The 33 internal coordinates listed in Table III which define the sets of M–Cl_t (r_i) and M–Cl_b (R_i) bond stretches and Cl_b–M–Cl_t (α_i), Cl_b–M–Cl_b (β_i), and M–Cl_b–M (θ_i) angle deformations were used, with standard group theoretical techniques, to generate the 33 symmetry coordinates[27] employed in this analysis. This over-definition of the problem (27 normal modes, 33 symmetry coordinates) produces six redundancies which appear as linear combinations of symmetry coordinates. The choice of the 33 internal coordinates listed in Table III minimizes the number of such redundancies in this analysis while, at the same time, it provides a convenient set of coordinates for the transfer of the results of this work to a subsequent analysis of metal cluster species. The relationship between those chosen and those useful in treating the cluster species is illustrated by Figure 4 in which the symbols bear the same meaning as in Figure 1. Note that β and β' are very similar but not identical in type.

The $Cr_2Cl_9^{3-}$ Ion.—The vibrational secular equation was solved with Schachtschneider's computer program[28] VSEC using symmetry-factored G and F matrices. The G matrix was calculated with Schachtschneider's GMAT program[28] using atomic distances and interatomic angles obtained from the crystal structure determination of $Cs_3Cr_2Cl_9$.[5] Redundancies were not removed from the G matrix, and produced zero roots to the secular equation. The redundancies also produce inherent ambiguities in the numerical values of several of the symmetrized force constants, $F_{i,j}^{\gamma}$, listed in Table IV. For example, the redundancy condition in the A_1' symmetry block requires that only the value of the linear combination $(F_{4,4} + n^2F_{5,5} - 2nF_{4,5})$, n = 1.03439, can be determined and not the values of the individual terms.

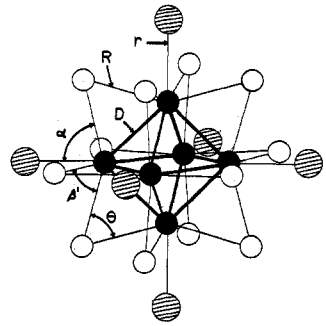

Figure 4.—The structure assumed by $[M_6Cl_{12}]X_6^{n-}$ ions, such as $[Nb_6Cl_{12}]Cl_6^{2-}$, with internal coordinate definitions that are marked by analogy with the internal coordinate set employed for the $M_2Cl_9^{3-}$ analysis. The filled circles represent the metal atoms in the octahedral cluster; the bridging chlorine atoms above the octahedral edges are unshaded; the terminal halogen atoms (X), one of which is attached to each metal atom in a centrifugal position, are hatched.

An initial symmetrized force field was constructed employing the values of k_{Cr-Cl}, $k_{Cl-Cr-Cl}$, and $k_{Cr-Cl,Cl-Cr-Cl}$ reported for CrO_2Cl_2,[29] the arithmetic relationships among the various valence force constants as used in the approximate analysis of $Cs_3Tl_2Cl_9$,[24] and the equations listed in Table IV. In addition, valence interaction force constants between M–Cl_t stretches on one end of the ion and all internal coordinates on the other end were set equal to zero. This requires $F_{1,j}^{A_1'} = F_{1,j}^{A_2''}$ and $F_{1,j}^{E'} = F_{1,j}^{E''}$. The symmetrized force field was then refined by analysis of the calculated eigenvectors to obtain good agreement between the calculated frequencies and those observed in the spectrum of $Cs_3Cr_2Cl_9$. Of the many solutions to the vibrational secular equation, several force fields were obtained for which the calculated–observed agree-

(26) E. B. Wilson, Jr., J. C. Decius, and P. C. Cross, "Molecular Vibrations," McGraw-Hill, New York, N. Y., 1955.

(27) A list of the symmetry coordinates used in this analysis will appear following these pages in the microfilm edition of this volume of the journal. Single copies may be obtained from the Business Operations Office, Books and Journals Division, American Chemical Society, 1155 Sixteenth St., N.W., Washington, D. C. 20036, by referring to code number INORG-72-2796. Remit check or money order for $3.00 for photocopy or $2.00 for microfiche.

(28) J. H. Schachtschneider, Technical Reports No. 231-64 and 57-65, Shell Development Co., Emeryville, Calif.

(29) H. Stammreich, K. Kawai, and Y. Tavares, *Spectrochim. Acta*, 438 (1959).

TABLE IV

FORCE FIELD FOR $Cr_2Cl_9^{3-}$ AND $W_2Cl_9^{3-}$ IONS

$F_{i,j}^{A_1'}$	$F_{i,j}^{A_2'}$	Composition of $F_{i,j}^{\gamma}$ in terms of internal valence force constants[a,b]	$Cr_2Cl_9^{3-}$		$W_2Cl_9^{3-}$	
			$F_{i,j}^{A_1'}$	$F_{i,j}^{A_2''}$	$F_{i,j}^{A_1'}$	$F_{i,j}^{A''}$
$F_{1,1}$	$F_{1,1}$	$k_{r1r1} \pm k_{r1r2} + 2k_{r1r3} \pm 2k_{r1r4}$	1.482	1.482	1.64	1.64
$F_{2,2}$	$F_{2,2}$	$k_{R1R1} \pm k_{R1R2} + 2k_{R1R3} \pm 2k_{R1R4}$	1.136	0.723	0.911	1.13
$F_{3,3}$	$F_{3,3}$	$k_{\alpha1\alpha1} + k_{\alpha1\alpha2} \pm k_{\alpha1\alpha3} \pm k_{\alpha1\alpha4} \pm 2k_{\alpha1\alpha5} + k_{\alpha1\alpha6} \pm 2k_{\alpha1\alpha7} \pm k_{\alpha1\alpha8} + k_{\alpha1\alpha10} \pm k_{\alpha1\alpha12}$	0.33	0.50	0.3276	0.545
$F_{4,4}$	$F_{4,4}$	$k_{\beta1\beta1} \pm k_{\beta1\beta2} + 2k_{\beta1\beta3} \pm 2k_{\beta1\beta4}$	0.146	0.32	0.146	0.32
$F_{5,5}$		$k_{\theta1\theta1} + 2k_{\theta1\theta2}$	0.126		0.126	
$F_{6,6}$		k_{M-M}			1.18	
$F_{1,2}$	$F_{1,2}$	$k_{r1R1} \pm k_{r1R2} + 2k_{r1R3} \pm 2k_{r1R4}$	0.353	0.353	0.44	0.44
$F_{1,3}$	$F_{1,3}$	$\sqrt{2}(k_{r1\alpha1} \pm k_{r1\alpha3} + k_{r1\alpha5} + k_{r1\alpha6} \pm k_{r1\alpha7} \pm k_{r1\alpha8})$	0.11	0.11	0.11	0.11
$F_{1,4}$	$F_{1,4}$	$k_{r1\beta1} \pm k_{r1\beta2} + 2k_{r1\beta3} \pm 2k_{r1\beta4}$	0.0	0.0	0.0	0.0
$F_{1,5}$		$\sqrt{2}(k_{r1\theta1} + 2k_{r1\theta2})$	−0.0122		−0.0122	
$F_{1,6}$		$\sqrt{6}(k_{r1,M-M})$			−0.2939	
$F_{2,3}$	$F_{2,3}$	$\sqrt{2}(k_{R1\alpha1} \pm k_{R1\alpha3} + k_{R1\alpha5} + k_{R1\alpha6} \pm k_{R1\alpha7} \pm k_{R1\alpha8})$	0.15	−0.14	0.15	−0.14
$F_{2,4}$	$F_{2,4}$	$k_{R1\beta1} \pm k_{R1\beta2} + 2k_{R1\beta3} \pm 2k_{R1\beta4}$	0.0443	0.10	0.0443	0.10
$F_{2,5}$		$\sqrt{2}(k_{R1\theta1} + 2k_{R1\theta2})$	0.1057		0.1057	
$F_{2,6}$		$\sqrt{6}(k_{R1,M-M})$			0.147	
$F_{3,4}$	$F_{3,4}$	$\sqrt{2}(k_{\alpha1\beta1} \pm k_{\alpha1\beta2} + k_{\alpha1\beta3} \pm k_{\alpha1\beta4} + k_{\alpha1\beta5} \pm k_{\alpha1\beta6})$	0.096	0.14	0.096	0.14
$F_{3,5}$		$2(k_{\alpha1\theta1} + k_{\alpha1\theta2} + k_{\alpha1\theta3})$	−0.04		−0.04	
$F_{3,6}$		$\sqrt{12}(k_{\alpha1,M-M})$			0.052	
$F_{4,5}$		$\sqrt{2}(k_{\beta1\theta1} + 2k_{\beta1\theta2})$	0.02		0.02	
$F_{4,6}$		$\sqrt{6}(k_{\beta1,M-M})$			0.0627	
$F_{5,6}$		$\sqrt{3}(k_{\theta1,M-M})$			0.0745	
$F_{1,1}^{A_1''}$	$F_{1,1}^{A_2}$	$(k_{\alpha1\alpha1} - k_{\alpha1\alpha2} \pm k_{\alpha1\alpha3} \pm k_{\alpha1\alpha4} + 2k_{\alpha1\alpha5} - k_{\alpha1\alpha6} \pm 2k_{\alpha1\alpha7} \pm k_{\alpha1\alpha8} - k_{\alpha1\alpha10} \pm k_{\alpha1\alpha12})$	$F_{1,1}^{A_1''}$ 0.035[d]	$F_{1,1}^{A_2'}$ 0.035[d]	$F_{1,1}^{A_1''}$ 0.03[d]	$F_{1,1}^{A_2'}$ 0.03[d]
$F_{i,j}^{E'}$	$F_{i,j}^{E''}$		$F_{i,j}^{E'}$	$F_{i,j}^{E''}$	$F_{i,j}^{E'}$	$F_{i,j}^{E''}$
$F_{1,1}$	$F_{1,1}$	$k_{r1r1} \pm k_{r1r2} - k_{r1r3} \pm k_{r1r4}$	1.09	1.09	1.30	1.30
$F_{2,2}$	$F_{2,2}$	$k_{R1R1} \pm k_{R1R2} - k_{R1R3} \pm k_{R1R4}$	0.686	0.72	0.63	1.32
$F_{3,3}$	$F_{3,3}$	$k_{\alpha1\alpha1} + k_{\alpha1\alpha2} \pm k_{\alpha1\alpha3} \pm k_{\alpha1\alpha4} - k_{\alpha1\alpha5} \pm k_{\alpha1\alpha7} - {}^1/_2(k_{\alpha1\alpha6} \pm k_{\alpha1\alpha8} + k_{\alpha1\alpha10} \pm k_{\alpha1\alpha12})$	0.282	0.11	0.145	0.131
$F_{4,4}$	$F_{4,4}$	$k_{\alpha1\alpha1} - k_{\alpha1\alpha2} \pm k_{\alpha1\alpha3} \pm k_{\alpha1\alpha4} - k_{\alpha1\alpha5} \pm k_{\alpha1\alpha7} + {}^1/_2(k_{\alpha1\alpha6} \pm k_{\alpha1\alpha8} + k_{\alpha1\alpha10} \pm k_{\alpha1\alpha12})$	0.242	0.263	0.185	0.237
$F_{5,5}$	$F_{5,5}$	$k_{\beta1\beta1} \pm k_{\beta1\beta2} - k_{\beta1\beta3} \pm k_{\beta1\beta4}$	0.14	0.12	0.14	0.12
$F_{6,6}$		$k_{\theta1\theta1} - k_{\theta1\theta2}$	0.10		0.10	
$F_{1,2}$	$F_{1,2}$	$k_{r1R1} \pm k_{r1R2} - k_{r1R3} \pm k_{r1R4}$	0.09	0.09	−0.07	−0.07
$F_{1,3}$	$F_{1,3}$	$1/\sqrt{2}(2k_{r1\alpha1} \pm 2k_{r1\alpha3} - k_{r1\alpha5} - k_{r1\alpha6} \pm k_{r1\alpha7} \pm k_{r1\alpha8})$	−0.03	−0.03	−0.03	−0.03
$F_{1,4}$[c]	$F_{1,4}$[c]	$\sqrt{3/2}(k_{r1\alpha5} - k_{r1\alpha6} \pm k_{r1\alpha7} \pm k_{r1\alpha8})$	0.0	0.0	0.0	0.0
$F_{1,5}$	$F_{1,5}$	$k_{r1\beta1} \pm k_{r1\beta2} - k_{r1\beta3} \pm k_{r1\beta4}$	0.0	0.0	0.0	0.0
$F_{1,6}$		$\sqrt{2}(k_{r1\theta1} - k_{r1\theta2})$	0.0		0.0	
$F_{2,3}$	$F_{2,3}$	$1/\sqrt{2}(2k_{R1\alpha1} \pm 2k_{R1\alpha3} - k_{R1\alpha5} - k_{R1\alpha6} \pm k_{R1\alpha7} \pm k_{R1\alpha8})$	0.123	0.05	0.123	0.05
$F_{2,4}$[c]	$F_{2,4}$[c]	$\sqrt{3/2}(k_{R1\alpha5} - k_{R1\alpha6} \pm k_{R1\alpha7} \pm k_{R1\alpha8})$	0.0	0.0	0.0	0.0
$F_{2,5}$	$F_{2,5}$	$k_{R1\beta1} \pm k_{R1\beta2} - k_{R1\beta3} \pm k_{R1\beta4}$	0.02	0.03	0.02	0.03
$F_{2,6}$		$\sqrt{2}(k_{R1\theta1} - k_{R1\theta2})$	−0.03		−0.03	
$F_{3,4}$[c]	$F_{3,4}$[c]	$-\sqrt{3/4}(k_{\alpha1\alpha6} \pm k_{\alpha1\alpha8} - k_{\alpha1\alpha10} \pm k_{\alpha1\alpha12})$	−0.03	−0.07	0.013	−0.04
$F_{3,5}$	$F_{3,5}$	$1/\sqrt{2}(2k_{\beta1\alpha1} \pm 2k_{\beta1\alpha3} - k_{\beta1\alpha5} - k_{\beta1\alpha6} \pm k_{\beta1\alpha7} \pm k_{\beta1\alpha8})$	0.0	0.0	0.0	0.0
$F_{3,6}$		$2k_{\alpha1\theta1} - k_{\alpha1\theta2} - k_{\alpha1\theta3}$	−0.05		−0.05	
$F_{4,5}$[c]	$F_{4,5}$[c]	$\sqrt{3/2}(k_{\beta1\alpha5} - k_{\beta1\alpha6} \pm k_{\beta1\alpha7} \pm k_{\beta1\alpha8})$	0.054	−0.03	0.054	−0.03
$F_{4,6}$[c]		$-\sqrt{3}(k_{\alpha1\theta2} - k_{\alpha1\theta3})$	0.0		0.0	
$F_{5,6}$		$\sqrt{2}(k_{\beta1\theta1} - k_{\beta1\theta2})$	−0.02		−0.02	

[a] The upper signs generate the $F_{i,j}^{A_1'}$ ($F_{i,j}^{E'}$) and the lower signs generate the $F_{i,j}^{A_2''}$ ($F_{i,j}^{E''}$). [b] For the $F_{i,j}^{E'}$ and $F_{i,j}^{E''}$, $F_{iz,jz}^{\gamma} = F_{iy,jy}^{\gamma}$ except where noted. See footnote *c*. [c] $F_{iz,jz}^{\gamma} = -F_{iy,jy}^{\gamma}$. [d] Assumed values. Using these values, the frequencies of the A_1'' and A_2' inactive modes are calculated to be 41 and 70 cm^{-1} (Cr) and 42 and 68 cm^{-1} (W).

ment is good, the individual $F_{i,j}^{\gamma}$ retain physically reasonable values, and the potential energy distribution of each of the calculated modes is consistent with the vibrational assignments. Each of these fields was employed in the $W_2Cl_9^{3-}$ analysis, as discussed below, and the one listed in Table IV results from the simultaneous treatment of these ions.

The $W_2Cl_9^{3-}$ Ion.—The results of the analysis of the $Cr_2Cl_9^{3-}$ ion were used as the basis of the analysis of the $W_2Cl_9^{3-}$ ion. The tungsten–tungsten stretching coordinate, S_{34}, was added to the set of internal coordinates, Table III, and becomes symmetry coordinate $S_6^{A_1'}$.[27] The G matrix was calculated using structural parameters obtained from the crystal structure determination of $K_3W_2Cl_9$,[11] and the several force fields obtained from the analysis of the $Cr_2Cl_9^{3-}$ ion were used as initial symmetrized F matrices. The E′ and E″ symmetry blocks were refined permitting only $F_{1,1}^{\gamma}$, $F_{2,2}^{\gamma}$, $F_{1,2}^{\gamma}$, $F_{3,3}^{\gamma}$, $F_{4,4}^{\gamma}$, and $F_{3,4}^{\gamma}$ to vary from the $Cr_2Cl_9^{3-}$ values while retaining the additional constraint of $F_{1,j}^{E'} = F_{1,j}^{E''}$.

The presence of the additional symmetry coordinate, $S_6^{A_1'}$, produces an additional redundancy in the A_1' symmetry block which involves the W–W stretching coordinate and makes the values of the W–W stretching force constant, $F_{6,6}^{A_1'} = k_{W-W}$, and the force constants

for the coordinates with which it is redundant physically ambiguous. However, the A_1' and A_2'' symmetry blocks were refined and the range of values of k_{W-W} determined as follows. With the values of the $F_{i,j}^{\gamma}$ from each of the several $Cr_2Cl_9^{3-}$ force fields and the initial values of the $F_{i,6}^{A_1'}$ (i = 1–6) set equal to zero, the calculated values of ν_1, which is relatively insensitive to the value of $F_{6,6}^{A_1'}$, and ν_7 were fit to the observed $K_3W_2Cl_9$ frequencies with $F_{1,1}^{\gamma}$ and $F_{1,2}^{\gamma}$, requiring that $F_{1,1}^{A_1'} = F_{1,1}^{A_2''}$ and $F_{1,2}^{A_1'} = F_{1,2}^{A_2''}$. The calculated values of ν_4, which is also insensitive to $F_{6,6}^{A_1'}$, ν_8, and ν_9 were fit to the observed values with $F_{3,3}^{A_1'}$, $F_{2,2}^{A_2''}$, and $F_{3,3}^{A_2''}$, respectively. Finally, the values of ν_2 and ν_3, both of which involve deformations of the bridging unit, were fit to the observed frequencies with $F_{2,2}^{A_1'}$, $F_{6,6}^{A_1'}$, and its associated interactions $F_{6,j}^{A_1'}$. Thus, $F_{6,6}^{A_1'}$ ($=k_{W-W}$) is determined within these assumptions and, from the range of values calculated by this procedure, is assigned the value k_{W-W} = 1.15 ± 0.1 mdyn/Å.

The force fields tabulated in Table IV provided excellent agreement between observed and calculated frequencies—agreement was within 1 cm^{-1} for all modes—for both the $Cr_2Cl_9^{3-}$ and $W_2Cl_9^{3-}$ ions, and yielded a value of k_{W-W} = 1.18 mdyn/Å. Subsequent decomposition of these values using the equations given in Table IV produced a set of internal valence force constants, selected values of which are listed in Table V.

TABLE V
VALUES OF SELECTED INTERNAL VALENCE FORCE CONSTANTS[a]

	Cr	W		Cr, W[b]
$k_{r_1r_1}$	1.22	1.41	$k_{R_1\beta_1}$	0.04
$k_{r_1r_3}$	0.13	0.11	$k_{R_1\beta_2}$	−0.01
$k_{R_1R_1}$	0.78	0.99	$k_{R_1\beta_3}$	0.02
$k_{R_1R_2}$	0.06	−0.27	$k_{R_1\beta_4}$	−0.01
$k_{R_1R_3}$	0.08	0.02	$k_{R_1\theta_1}$	0.01
$k_{R_1R_4}$	0.07	0.08	$k_{R_1\theta_2}$	0.03
$k_{r_1R_1}$	0.18	0.10	$k_{\beta_1\beta_1}$	0.16
$k_{r_1R_3}$	0.09	0.18	$k_{\beta_1\beta_2}$	−0.02
$k_{\alpha_1\alpha_1}$	0.22	0.19	$k_{\beta_1\beta_3}$	0.03
k_{M-M}		1.18	$k_{\beta_1\beta_4}$	−0.03
k_{rM}		−0.12	$k_{\theta_1\theta_1}$	0.11
k_{RM}		0.06	$k_{\theta_1\theta_2}$	0.01
$k_{\beta M}$		0.03	$k_{\beta_1\theta_1}$	−0.005
$k_{\theta M}$		0.04	$k_{\beta_1\theta_2}$	0.01

[a] Values in mdyn/Å obtained from Table IV. [b] Same numerical values used for the analysis of both complex ions.

While a comparison of the values of the internal valence force constants obtained from this work with previously reported studies is difficult, both because of the limited number of such studies and because of the basic structural and electronic differences that must be considered in making such comparisons, several features bear comment. A normal coordinate analysis of chromyl chloride, CrO_2Cl_2,[29] yielded values of 0.21 and 0.04 mdyn/Å for $k_{Cl-Cr-Cl}$ and $k_{Cr-Cl,Cl-Cr-Cl}$, respectively, with which our values of k_{α_1,α_1} (~0.22) and k_{r_1,α_5} (~0.03) compare favorably. Unfortunately, a normal-coordinate treatment of the $CrCl_6^{3-}$ ion, with which more meaningful comparisons might be made, has not been reported to date. The hexachlorides of tungsten provide a more convenient set of force constants to which our results for $K_3W_2Cl_9$ can be compared. The several treatments of WCl_6^n (n = 0, −1, −2)[30] have yielded values of k_{W-Cl} from >2.0 (n = 0) to ~1.6 mdyn/Å (n = −2); our value of $k_{r_1,r_1} \simeq 1.4$ mdyn/Å follows this trend of decreasing force constant value with decrease of tungsten formal oxidation state. Our value of $k_{\alpha_1,\alpha_1} \simeq 0.19$ mdyn/Å also agrees well with the average of the values of $k_{Cl-W-Cl}$ (0.20 mdyn/Å).

Discussion

The results of this study of the vibrational spectra of $Cr_2Cl_9^{3-}$ and $W_2Cl_9^{3-}$ ions address two outstanding problems in the study of metal–metal bonded compounds. The first is the vibrational analysis of spectra of metal cluster species, such as those of general formula $M_6X_8^n$ (*e.g.*, $(W_6Cl_8)Cl_4$) and those of the type $[M_6Y_{12}]X_6$ (*e.g.*, $[Nb_6Cl_{12}]Cl_6^{2-}$). The goal of such analyses is determination of the magnitude of metal–metal interaction, generally in the form of a force constant for small amplitude displacement along a given metal–metal coordinate. The second is the nature of the bonding in the $W_2Cl_9^{3-}$ ion, which exhibits only weak temperature-independent paramagnetism.

In the case of $W_2Cl_9^{3-}$ the existence of bridging atoms connecting the metal atoms in a way sufficient to formally account for the molecular structure introduces vibrational coordinate redundancy between the bridge angles and the intermetallic distention. This redundancy is the essence of the vibrational analysis problem in the case of the $[M_6Cl_{12}]X_6$ cluster shown in Figure 4, which illustrates the correspondence between the types of internal coordinates employed for $W_2Cl_9^{3-}$ and those useful in the analysis of cluster species. The vibrational coordinate redundancy introduces an essential ambiguity into the force field which rigorously precludes the individual determination of either the angle change force constants or the metal–metal distention force constant in the vibrational analysis of any single isotopic molecule. The only mathematically acceptable solution to this difficulty (other than tolerating the ambiguity) is to assume the values of certain portions of the force field and determine the remaining ones. Two useful *a priori* assumptions that can be made are (1) the force field elements associated with one redundant coordinate set are zero (a key assumption in the $Cr_2Cl_9^{3-}$ case) or (2) that the values of the force field elements for one such set can be estimated on the basis of other information. In this study we have taken the approach of assuming that the force-field elements for angle distortions of the bridging framework contributing to A_1' modes in $Cr_2Cl_9^{3-}$ can be transferred to the $W_2Cl_9^{3-}$ case. This allows the angle bend–metal–metal stretch redundancy to be tolerated and the value of k_{W-W} to be determined (to within the accuracy of the assumption). The good calculated–observed agreement this transfer leads to throughout the spectrum is encouraging evidence for the validity of this assumption, but we recognize that this could be an artifact of the values taken for several off-diagonal F matrix elements.

The key point is that a rather good determination of the potential energy partitioning between the metal–metal stretch and the angle bends can be made without demanding *perfect* transferability of the angle distor-

(30) T. L. Brown, W. G. McDugle, Jr., and L. G. Kent, *J. Amer. Chem. Soc.*, **92**, 3645 (1970), and references therein.

tion force constants. This partitioning, or potential energy pattern, then becomes a criterion for dealing with force constant ambiguities in the cluster molecule cases. It can be seen most readily by comparing the components of the potential energy distribution for modes ν_3 and ν_4 of A_1' type of both $Cr_2Cl_9^{3-}$ and $W_2Cl_9^{3-}$ in Table VI. As is to be expected, the bridge

TABLE VI

POTENTIAL ENERGY CONTRIBUTION OF THE $F_{i,j}^{A_1}$ TO THE CALCULATED A_1' MODES OF $M_2Cl_9^{3-}$

	ν, cm^{-1} calcd = obsd ±1	$Cr_2Cl_9^{3-}$ (% contribution of $F_{i,j}^{A_1'}$)	ν, cm^{-1} calcd = obsd ±1	$W_2Cl_9^{3-}$ (% contribution of $F_{i,j}^{A_1'}$)
ν_1	375	$F_{1,1}$(72), $F_{2,2}$(32), $F_{1,2}$(−26)	331	$F_{1,1}$(77)
ν_2	280	$F_{1,1}$(14), $F_{2,2}$(82), $F_{1,2}$(18), $F_{2,3}$(−13)	257	$F_{2,2}$(98), $F_{3,3}$(11), $F_{2,3}$(−12)
ν_3	161	$F_{1,1}$(23), $F_{4,4}$(47), $F_{5,5}$(38), $F_{4,5}$(−12)	139	$F_{1,1}$(39), $F_{2,2}$(35), $F_{4,4}$(35), $F_{5,5}$(36), $F_{6,6}$(44), $F_{1,2}$(−26), $F_{1,6}$(−17), $F_{2,5}$(−22), $F_{2,6}$(−11), $F_{4,5}$(−10), $F_{4,6}$(−11), $F_{5,6}$(15)
ν_4	121	$F_{3,3}$(139), $F_{4,4}$(35), $F_{5,5}$(28), $F_{3,4}$(−61), $F_{3,5}$(−25)	115	$F_{3,3}$(125), $F_{3,3}$(−15), $F_{3,4}$(−16)

and skeletal angle distortions mix extensively in ν_3 and ν_4 for $Cr_2Cl_9^{3-}$, since they are of similar frequency. The introduction of a value for $F_{6,6}^{A_1'}$ (k_{W-W}) sufficient to bring ν_3 to its assigned value leaves the contributions from the bridge angle distortions nearly unchanged, but causes the contribution of the terminal angles to diminish in ν_3 and increase in ν_4. This partitioning of bridge from terminal distortions is only slightly affected by the assumed values of $F_{6,j}^{A_1'}$, as shown by several computations in which introduction of k_{W-W} was accomplished with different combinations of $F_{6,6}^{A_1'}$ and $F_{6,j}^{A_1'}$, subject only to the constraint that $0.25F_{6,6}^{A_1'} > |F_{6,j}^{A_1'}|$. On the basis of these results it is expected that calculation of k_{M-M} for even rather strong metal–metal bonds must be accompanied by reasonable assumptions for the force field elements for angle distortions if the resultant values of k_{M-M} are to be accurate to within even a factor of 2. The relative contributions of each internal coordinate-type to be expected may be estimated from the values in Table VI.

The nature of the bonding of $W_2Cl_9^{3-}$ has been the subject of considerable interest and speculation since its structure[30] and low magnetic moment were first determined. The currently accepted magnetic measurements[8,12] indicate a temperature-independent paramagnetic moment of 0.47 BM. Since the W atoms formally have a d^3 configuration, extensive spin coupling is indicated, but the extent to which this is due to direct metal–metal bond formation has not been conclusively demonstrated. Formally, of course, W–W triple bond formation can lead to diamagnetism or temperature-independent paramagnetism, and this has frequently been forwarded as a bonding rationale. Pauling[31,32] has postulated a W–W bond order of two for $W_2Cl_9^{3-}$.

(31) C. Brossett, *Ark. Kemi., Mineral. Geol.*, **12**, 4 (1935).

(32) L. Pauling, "The Nature of the Chemical Bond," 3rd ed, Cornell University Press, Ithaca, N. Y., 1960, p 437.

The value of k_{W-W} reported here is interesting to consider in light of such bonding arguments and the values of other metal–metal bond force constants. The value of k_{W-W} of 1.15 mdyn/Å is somewhat higher than those for unsupported metal–metal single bonds involving group VIb elements. Thus, k_{Mn-Cr} ($MnCr(CO)_{10}^-$ is 0.51, and k_{Mn-W} ($MnW(CO)_{10}^-$) is 0.77 mdyn/Å (3d). Comparison of these species with $W_2Cl_9^{3-}$ is tenuous, but it does indicate that while the W–W bond order is between one and two, it is much weaker than would be expected for a triple bond. It seems clear, therefore, that a spin-coupling mechanism which does not involve W–W triple bond formation is required. In this regard, the studies of Smith, *et al.*,[7,33] and of Wentworth, *et al.*,[34] on $Mo_2Cl_9^{3-}$ are interesting to consider, along with the bonding discussions of Wentworth, *et al.*,[6] and Cotton, *et al.*[35,36]

In studying the relative contributions of the different mechanisms for spin coupling in $Mo_2Cl_9^{3-}$ salts, which exhibit small temperature-dependent paramagnetism and are thus intermediate between $Cr_2Cl_9^{3-}$ and $W_2Cl_9^{3-}$ in magnetic susceptibility, Grey and Smith[7] showed that direct exchange predominates and superexchange *via* bridging halogens accounts for only a minor portion of the total exchange. While superexchange is comparable in magnitude with direct exchange for the corresponding $Cr_2Cl_9^{3-}$, the total exchange in these cases is about 50 times smaller than in the $Mo_2Cl_9^{3-}$ salts. By extension, the low magnetic moment of $W_2Cl_9^{3-}$ would be predominantly a result of direct exchange. Several reasonable postulates have been proposed to account for the $W_2Cl_9^{3-}$ structural and magnetic data, of which one[6] involves three W–W bond interactions from direct overlap of the half-filled "t_{2g}" orbitals on the adjacent W atoms. The other[6] postulated "direct overlap of only the trigonally directed d_{z^2} orbitals on adjacent W atoms," leading to a single interaction, with the remaining electrons "located in either localized pairs or in singly occupied, localized orbitals with interionically coupled spins." In either event, the expectation[35] of submaximal overlap in at least two of these bonding interactions is borne out by our finding that the W–W force constant k_{W-W} is inconsistent with three W–W bonds of maximal overlap. Indeed, the value of k_{W-W} reported here is most consistent with a W–W bond order a bit greater than one.

Acknowledgment.—We gratefully acknowledge the support of this work by the Advanced Research Projects Agency under Contract SD-86 with Brown University. The laser Raman instrument purchase was made possible through Grant GP-10187 from the National Science Foundation. Acknowledgment is made to the donors of the Petroleum Research Fund, American Chemical Society, for partial support of this research.

(33) I. E. Grey and P. W. Smith, *Aust. J. Chem.*, **22**, 121 (1969).

(34) R. Saillant and R. A. D. Wentworth, *Inorg. Chem.*, **8**, 1226 (1969).

(35) F. A. Cotton, *Rev. Pure Appl. Chem.*, **27**, 25 (1967).

(36) M. J. Bennett, J. V. Brencic, and F. A. Cotton, *Inorg. Chem.* **8**, 1060, (1969); and private communication reported in ref 6.